BOLETIN DE LA SOCIEDAD ESPAÑOLA DE
Cerámica y Vidrio
www.elsevier.es/bsecv

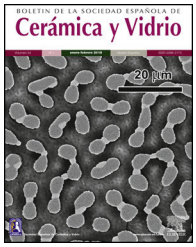

Original

Fluorine-induced in situ crystallization route to mesoporous $Li_2Si_2O_5$ hydrate dumbbell-like structures

*Hui Zhang, Jinxiao Wang, Jianfeng Yang**

State Key Laboratory for Mechanical Behavior of Materials, Xi'an Jiaotong University, Xi'an 710049, China

ARTICLE INFO

Article history:
Received 18 June 2019
Accepted 11 September 2019
Available online 22 October 2019

Keywords:
NH_4F
Hydrothermal synthesis
$Li_2Si_2O_5$ hydrate dumbbells
Methylene blue adsorption

ABSTRACT

Herein, mesoporous $Li_2Si_2O_5$ hydrate dumbbell-like structures were for the first time fabricated by a fluorine-induced in situ crystallization route. The obtained dumbbells assembled by nanowire-nanoparticles featured highly porous structures with mesoporous pores below 13 nm, enabling a remarkably large surface area of 76.71 $m^2 \cdot g^{-1}$ which was 4.09 times that of the structures in NH_4F-free solution and represented one of highest values reported to date on $Li_2Si_2O_5$ structures. The novel mesoporous structures revealed a new strategy to enhance the methylene blue adsorbance to 66.09 $mg\,g^{-1}$, allowing for their promising functional application in effluent treatment.

© 2019 Published by Elsevier España, S.L.U. on behalf of SECV. This is an open access article under the CC BY-NC-ND license (http://creativecommons.org/licenses/by-nc-nd/4.0/).

Ruta de cristalización in situ inducida por flúor a estructuras de hidrato de $Li_2Si_2O_5$ mesoporoso en forma de mancuernas

Palabras clave:
NH_4F
Síntesis hidrotérmica
Mancuernas de hidrato de $Li_2Si_2O_5$
Adsorción de azul de metileno

RESUMEN

Aquí, un hidrato de $Li_2Si_2O_5$ mesoporoso en forma de mancuernas fue obtenido por primera vez usando una ruta de cristalización in situ inducida por flúor. Las mancuernas obtenidas, formadas por el ensamblaje de nanopartículas en forma de nanohilos, presentaron una porosidad elevada, con mesoporos por debajo de los 13 nm, habilitando un área superficial particularmente grande, de 76,71 $m^2 \cdot g^{-1}$, siendo este valor 4,09 veces el de las estructuras obtenidas sin el empleo de NH4F, lo que representa uno de los valores más altos descritos hasta la fecha en estructuras de $Li_2Si_2O_5$. Las nuevas estructuras mesoporosas revelaron una estrategia novedosa para mejorar la adsorción de azul de metileno a 66,09 $mg \cdot g^{-1}$, lo que supone una prometedora aplicación en el tratamiento de efluentes.

© 2019 Publicado por Elsevier España, S.L.U. en nombre de SECV. Este es un artículo Open Access bajo la licencia CC BY-NC-ND (http://creativecommons.org/licenses/by-nc-nd/4.0/).

* *Corresponding author.*
E-mail address: yangjianfeng51@163.com (J. Yang).
https://doi.org/10.1016/j.bsecv.2019.09.004
0366-3175/© 2019 Published by Elsevier España, S.L.U. on behalf of SECV. This is an open access article under the CC BY-NC-ND license (http://creativecommons.org/licenses/by-nc-nd/4.0/).

Introduction

$Li_2Si_2O_5$ is considered to be one of the most promising functional materials in many areas, such as dentistry, CO_2 adsorption, tritium breeders and so on [1–3]. Research in these areas is closely related to the synthetically controlled morphologies that represent the key modulation in the properties of final products that largely determine the field of material capability [4–6]. Conventionally, direct solid-state reaction or chemical precipitation processes are the most common methods for obtaining granular $Li_2Si_2O_5$ powders [7,8]. However, these strategies are solely effective for relative dense $Li_2Si_2O_5$ bulk crystals without pores, because the rapidly short-length diffusion of lithium arouses compact surface layers formed on pristine particles. An alternative route is to deposit 2D sheet-like $Li_2Si_2O_5$ nanostructures through a mild hydrothermal process, which endows a useful function [9,10]. Despite the success in functional enhancements, it still faces problems of fairly low surface area, resulting in heavy loss of other functions. Up to now, little success has been achieved in constructing functional $Li_2Si_2O_5$ hierarchical structures owing to the difficulty in simultaneously controlling the growth of $Li_2Si_2O_5$ and their properties. Herein, we reported a fluorine-induced in situ crystallization route to synthesize a novel type of mesoporous dumbbell-like $Li_2Si_2O_5$ hydrate structures with large surface area and potential methylene blue (denoted as MB) adsorption function.

Experimental

Typically, a certain weight of NH_4F (0, 0.074, 0.148, 0.296, 0.592 g) was dissolved in 75 mL of deionized water and magnetically stirred, followed by addition of 0.2 M $LiOH{\cdot}H_2O$ and TEOS with Li/Si = 1. After vigorously stirring for 30 min, the solution was transferred into a 100 mL Teflon-lined autoclave and maintained at 180 °C for 48 h. The as-obtained white products were collected by washing several times with alcohol, and then dried at 80 °C for 24 h.

Results and discussion

Fig. 1 shows the morphological details and phase composition of the product prepared at 0.148 g NH_4F. The product presented dumbbell-like structure from the panoramic image (Fig. 1a). The two lobe brushes of the dumbbell radiated symmetrically from the center with diameter of about 2.5 μm, resulting in a total size of about 25 μm. It could be found that the brushes were constructed by flocky nanowires of about 200 nm (Fig. 1b). From the magnified TEM image and SAED patterns (Fig. 1c), it could be seen that the single flocky nanowire exhibited composite structure consisting of highly crystallized single-crystalline gracile nanowire with agglomerated polycrystalline nanoparticles coated on. Notably, the plenty of agglomerated nanoparticles formed a mesoporous

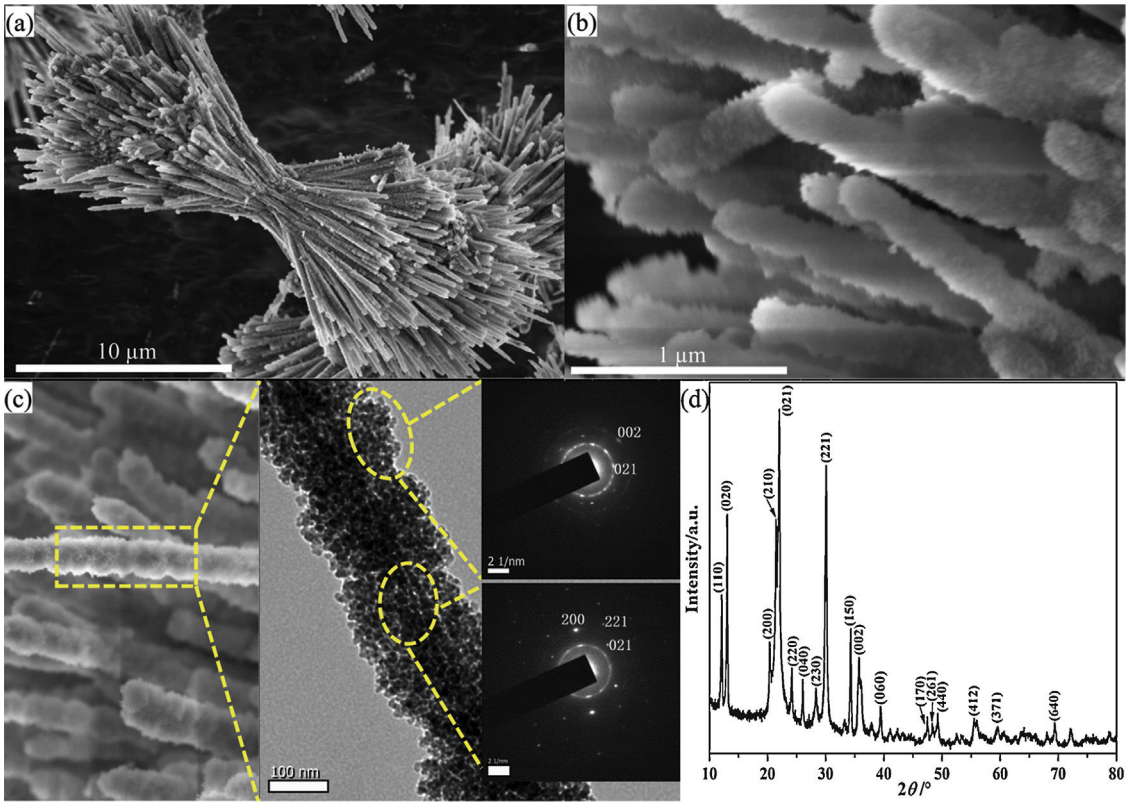

Fig. 1 – (a) The integral and (b) the high-magnification FE-SEM images, (c) the single nanowire and its corresponding TEM image, (d) XRD pattern of $Li_2Si_2O_5$ hydrate dumbbells prepared at 0.148 g NH_4F. Insets in (c) are the SAED patterns of two counterparts showing polycrystalline nanoparticles and single-crystal nanowire in the dumbbell, respectively.

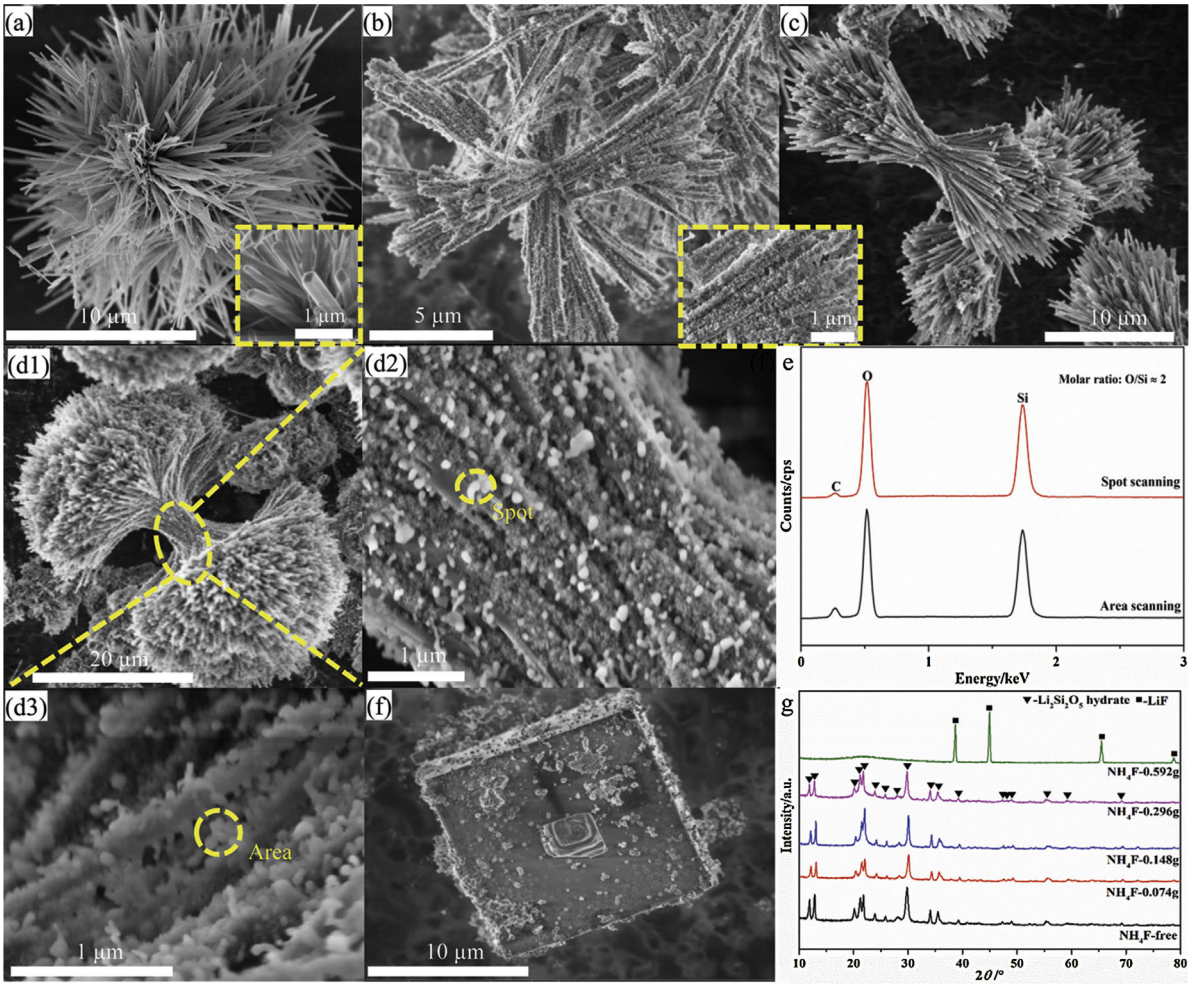

Fig. 2 – FE-SEM images and corresponding XRD patterns of $Li_2Si_2O_5$ hydrate products prepared at different NH_4F content: (a) 0, (b) 0.074, (c) 0.148 and (d) 0.296 g NH_4F, (e) corresponding spot and area EDS patterns in magnified views of d2 and d3, (f) 0.592 g NH_4F; and (g) the XRD patterns.

structure. The XRD peaks in Fig. 1(d) could be well indexed to the pure orthorhombic structure of $Li_2Si_2O_5$ hydrate crystals ($Li_2Si_2O_5{\cdot}2H_2O$) (JCPDS No. 33-0816), indicating a high crystallinity in consistent with the TEM result.

Fig. 2 shows the morphological evolution and phase composition of at different NH_4F content. In the absence of NH_4F, only $Li_2Si_2O_5$ hydrate clusters assembled by multi-directional prismatic rods radiating from the center were observed (Fig. 2a). Increasing the NH_4F content to 0.074 g, $Li_2Si_2O_5$ hydrate rod-nanoparticle composites were derived and packed together to form delicate brushes that were radially but symmetrically arranged and bundled at one center (Fig. 2b). Adjusting the content to 0.148 g, dumbbell-like $Li_2Si_2O_5$ hydrate structures that composed of two symmetrical lobes were formed (Fig. 2c). When 0.296 g NH_4F was introduced, the two lobes of the dumbbell derived into two hemispherical brushes with high-density nanowire-nanoparticles as shown in Fig. 2(d1). From the enlarged views (Fig. 2(d2–d3)), it could be visibly observed that numerous bigger white nanoparticles were adhered on the pristine $Li_2Si_2O_5$ hydrate nanoparticles. This might be ascribed to amorphous SiO_2 by the EDS results in Fig. 2(e), in agreement with the amorphous characteristics in the XRD domain peaks from 20 to 25° (Fig. 2(g)) that differed from the product at 0.148 g NH_4F. However, when 0.592 g NH_4F was introduced, only cubic LiF (JCPDS No. 04-0857, Fig. 2(g)) blocks were formed accompanied with a spot of amorphous SiO_2 (Fig. 2(f)).

Apparently, NH_4F played a decisive role in directing the $Li_2Si_2O_5$ hydrate structures. On the basis of previous studies [11–13], the growth of dumbbell-like structures was highly related to an in situ crystallization process that occurred solely along the crystal facet direction adsorbing fluorine due to the lower surface energy. In this process, NH_4F hydrolyzed into ammonia acting as a pH buffer to slowly release OH^- [14,15]. The surfaces of early formed $Li_2Si_2O_5$ hydrate nanowires were unsaturated charged and surface Li^+ could interact with fluorine to form Si-O-Li-F complexes as confirmed by the XPS spectra of surface composition containing O, Si, F and Li (Fig. S1). The hydrogen bonding between Si-O-Li-F complexes and ammonia in the solution made the complexes act as anchor sites to capture OH^-. OH^- exchanged with fluorine resulting in chemical defects that benefited heterogeneous nucleation on the nanowires [16–18]. The more the NH_4F content was, the more nucleation sites on the surfaces formed,

Table 1 – The BET parameters of dumbbell-like structures (0.148 g NH_4F) compared with rod clusters (NH_4F-free).

Parameters	Samples	With NH_4F	NH_4F-free
Specific surface area ($m^2 \cdot g^{-1}$)		76.71	18.74
Average pore diameter (nm)		12.46	13.92
Pore volume ($cm^3 \cdot g^{-1}$)		17.08×10^{-2}	4.84×10^{-2}

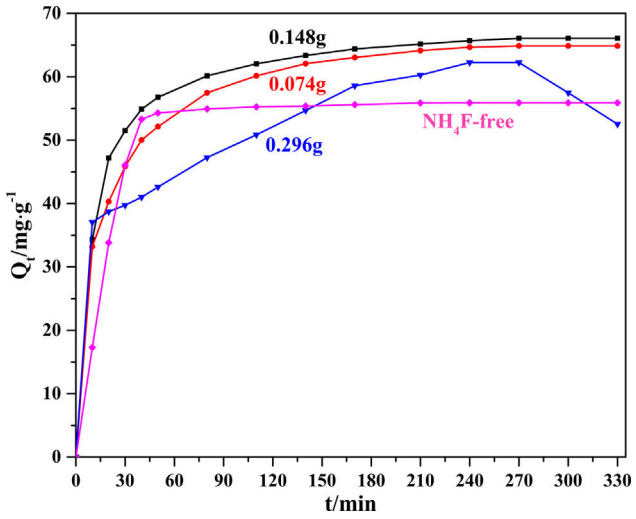

Fig. 3 – The MB adsorption curves of $Li_2Si_2O_5$ hydrate products prepared at different NH_4F content.

accelerating the nuclei deposition and leading to further quantities of nanowires derived (0.296 g) and vice versa (0.074 g). Importantly, excess consumption of OH^- by ammonia led to the surplus of TEOS due to $Li^+/OH^-/Si = 1$ for $Li_2Si_2O_5 \cdot 2H_2O$, thereby SiO_2 nanoparticles formed. When using 0.592 g NH_4F ($Li/F = 1$), the reaction between NH_4F and LiOH dominated because the supersaturation toward LiF was satisfied, resulting in a mixture of amorphous SiO_2 nanoparticles and highly crystallized LiF.

Table 1 compares the BET parameters of the dumbbells (0.148 g NH_4F) with the product of NH_4F-free. The specific surface area of the dumbbells was 76.61 $m^2 \cdot g^{-1}$, 4.09 times that of NH_4F-free product and higher than that of other related report [19]. The average pore diameter and pore volume were 12.46 nm and 17.08×10^{-2} $cm^3 \cdot g^{-1}$, respectively, indicating that the product was mesoporous material [20] in agreement with the TEM result.

Fig. 3 compares the MB adsorption kinetics of $Li_2Si_2O_5$ hydrate products at different NH_4F content. The MB adsorbance of all the products rose rapidly at the very beginning (0–20 min) due to the strong electrostatic interaction between chromophoric groups of MB and surfaces of $Li_2Si_2O_5$ hydrate and a large number of unoccupied vacant surface. Then the adsorption rate gradually slowed down until equilibrium (4 h) due to the remaining vacant surface sites were difficult to be occupied resulted from the steric barrier between MB molecules on the surface [21]. Distinctly, the adsorption rate of products at 0.296 g NH_4F was slower than that of other products and the MB desorption occurred after equilibrium. It might be explained that numerous amorphous SiO_2 strong adhesion on dumbbells might occupy the active sites and reduce the electrostatic interaction between MB molecules and $Li_2Si_2O_5$ hydrate surfaces. The MB equilibrium adsorbance of these products were 55.89 (NH_4F-free), 64.87 (0.074 g NH_4F), 66.09 (0.148 g NH_4F) and 62.26 mg/g^{-1} (0.296 g NH_4F), respectively. It could also be found that $Li_2Si_2O_5$ hydrate dumbbells (0.148 g NH_4F) showed the largest adsorbance attributed to the enlarged specific surface area owing to the cavities between nanoparticles and nanowires resulted porous structure, implying a potential application in effluent treatment.

Conclusion

Novel mesoporous $Li_2Si_2O_5$ hydrate dumbbell-like structures were conveniently synthesized by a facile fluorine-induced in situ crystallization route, which featured a largest specific surface area of 76.71 $m^2 \cdot g^{-1}$ ever reported to date on $Li_2Si_2O_5$ structures. Benefiting from its unique mesoporous structure, $Li_2Si_2O_5$ hydrate dumbbells presented a strong methylene blue adsorbance to 66.09 $mg\,g^{-1}$, offering attractive benefits for promising functional application in effluent treatment.

Acknowledgments

We thank the National Key R&D Program of China (Grant No. 2017YFB0310300), the National Natural Science Foundation of China (Grant No. 51672209) for the support of this work.

REFERENCES

[1] H. Lammert, M. Kunow, A. Heuer, Phys. Rev. Lett. 90 (2003) 215901.
[2] B.N. Nair, R.P. Burwood, V.J. Goh, K. Nakagawa, T. Yamaguchi, Prog. Mater. Sci. 54 (2009) 511–541.
[3] D. Cruz, S. Bulbulian, J. Nucl. Mater. 312 (2003) 262–265.
[4] Y. BMao, S.S. Wong, J. Am. Chem. Soc. 128 (2006) 8217–8226.
[5] A. Riss, T. Berger, S. Stankic, J. Bernardi, E. Knözinger, O. Diwald, Angew. Chem. Int. Ed. 47 (2008) 1496–1499.
[6] C.T. Dinh, Y. Seo, T.D. Nguyen, F. Kleitz, T.O. Do, Angew. Chem. Int. Ed. 51 (2012) 6608–6612.
[7] H. Pfeiffer, P. Bosch, S. Bulbulian, J. Nucl. Mater. 257 (1998) 309–317.
[8] P. Li, L.F. Francis, J. Mater. Sci. 30 (1995) 6192–6204.
[9] A. Alemi, S. Khademinia, M. Dolatyari, A. Bakhtiari, Int. Nano Lett. 2 (2012) 1–9.
[10] A. Alemi, S. Khademinia, S.W. Joo, M. Dolatyari, A. Bakhtiari, Int. Nano Lett. 3 (2013) 1–11.
[11] H.K. Wang, K.P. Dou, W.Y. Teoh, Y.W. Zhan, T.F. Hung, F.H. Zhang, J.Q. Xu, R.Q. Zhang, A.L. Rogach, Adv. Funct. Mater. 23 (2013) 4847–4853.
[12] H.M. Zhang, Y.H. Han, P.R. Liu, H. Yu, S.Q. Zhang, C.D. Yao, H.J. Zhao, Chem. Commun. 46 (2010) 8395–8397.
[13] G. Liu, H.G. Yang, X.W. Wang, L.N. Cheng, J. Pan, G.Q. Lu, H.M. Cheng, J. Am. Chem. Soc. 131 (2009) 12868–12869.
[14] P. Kollman, I. Kuntz, J. Am. Chem. Soc. 98 (1976) 8295–8296.
[15] Z. Wen, L.P. Zhu, L. Li, L.W. Sun, H. Cai, Z.Z. Ye, Dalton Trans. 42 (2013) 15551–15554.

[16] Y. Wang, H. Xia, L. Lu, J.Y. Lin, ACS Nano 4 (2010) 1425–1432.
[17] J. Jiang, J.H. Zhu, R.M. Ding, Y.Y. Li, J. Mater. Chem. 21 (2011) 15969–15974.
[18] W.M. Mei, J. Huang, L.P. Zhu, Z.Z. Ye, J. Mater. Chem. 22 (2012) 9315–9321.
[19] X.Y. Li, H.M. Yang, Cryst. Eng. Comm. 16 (2014) 4501–4507.
[20] A. Kamari, W.S. Wan Ngah, M.Y. Chong, M.L. Cheah, Desalination 249 (2009) 1180–1189.
[21] S. Senthilkumaar, P.R. Varatharajan, K. Porkodi, C.V. Subbhuraam, J. Colloid Interface Sci. 284 (2005) 78–82.